

COMBINED HYDRO-WIND POWER GENERATION

Joana Preto Fialho

Instituto Superior Técnico, Lisboa, Portugal

January 2018

Abstract

The fast growing of new renewable energies such as wind energy and its issues in terms of the intermittency of natural resource inspired this work to present a hydro pumped storage (HPS) solution in a close grid, as a way of overcoming that obstacle, by increasing the wind penetration levels, providing balance power and helping to control the grid voltage and frequency.

Similarly, to many hydro pumped storage systems that have been proposed on islands, this paper proposes a HPS facility according to Portugal meteorological and hydrological conditions. This facility would therefore integrate the energy generation of a nearby wind farm.

The first step was to conceive a preliminary design consisting of a concrete level dam and its associated hydraulic structures, as well as of a hydraulic circuit connected to a pumping and turbine stations. The next step was to develop the enterprise model was lastly, 8 cases studies were simulated.

For a given demand curve, the results indicated that in addition to the conventional power station being indispensable, its annual contribution is 12% of the energy demand, in the most favorable case, with hydropower and wind generation contributing 33% and 55 %, correspondingly. Also, in this scenario, the annual energy stored can achieve 94 % of the wind energy leftover, more than the 85% establish as threshold.

Keywords: Wind-hydro power plant, pumped hydro energy storage system, small hydro

1. Introduction

To establish the HPS system, an upper reservoir was conceived next to Douro river in municipality of Freixo Espada à Cinta. It was assumed that water exploitation of Douro has no impact in downstream hydropower plants. The hydropower facility was implanted at the north riverbank.

Chapter 2 presents the hydrological study concerning issues such as the storage capacity curve, the peak flow discharge and the ecological discharge and evaporation losses.

Chapter 3 introduces the preliminary design of the dam and its hydraulic structures (spillway, bottom outlet and water intakes), together with the hydraulic circuits design.

Chapter 4 describes the components of the power system and chapter 5 briefly describes the simulated model. Chapter 6 then discusses the annual operating results and the final chapter 7 summarizes the main conclusions.

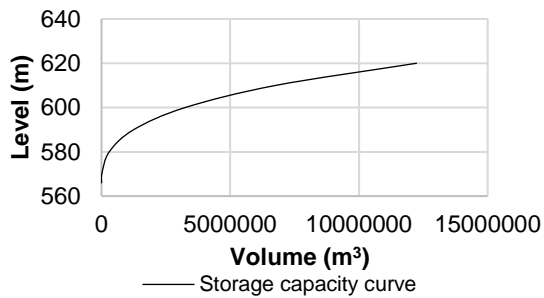
2. Hydrological study

The established watershed comprises an area of 3 km² and its the storage capacity curve is given by the Graphic 1.

To design the slipway structure, the design flood needs to be determined. Due to the small size of the watershed area, it was possible to apply the rational formula to find the 1000 years design peak runoff (Q). The formula relates the runoff-producing potential of the watershed (C), the

average intensity of rainfall (I) for a length of time in this case the time of concentration (t_c), and the watershed drainage area (A), corrected by an adjustment coefficient (C_f).

The storage capacity curve was abtained through the topographic maps of the area, the Carta Militar 142.

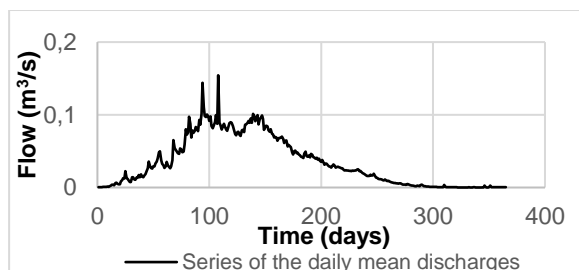


Graphic 1 – Storage capacity curve

Table 1- Rational formula

Q (m ³ /s)	65
I (mm/h)	122,24
t _c (min)	22
A (km ²)	3
C (-)	0,51
C _f (-)	1,25

To characterize the natural regime of the inflows of the study case, a transposition procedure was applied to the flow data acquired in one river gage station nearby the case study. The series is the daily average of flow data obtained by the previous procedure (Graphic 2), later applied in the simulated model.



Graphic 2 – Series of the daily mean discharges (Q_{nat})

The monthly time series concerning the evaporation phenomenon was computed by

applying a linear equation deduced by Martins (2016) that relates the potential evapotranspiration of Thornthwaite, and the evaporation (Table 2).

The ecological discharge was set equal to 5% of monthly average of the natural flow series (Table 2).

Table 2 - Evaporation losses and Ecological discharge

Months	Q _{evap} (m ³ /s)	Q _{eco} (m ³ /s)
Oct	2,50E-03	2,89E-04
Nov	1,14E-03	1,28E-03
Dec	6,16E-04	3,06E-03
Jan	4,90E-04	4,64E-03
Feb	6,33E-04	4,35E-03
Mar	1,41E-03	3,10E-03
Abr	2,07E-03	1,88E-03
May	3,28E-03	1,15E-03
Jun	4,51E-03	4,97E-04
Jul	6,02E-03	1,16E-04
Aug	5,50E-03	2,37E-05
Sep	3,86E-03	2,48E-05

3. Preliminary design of the dam and accessories

3.1. Reservoir and Dam - General Characteristics

The present work proposes a gravity concrete dam and placed according to the topography to maximize the water storage capacity as well as to minimize de axis length.

The dam body was established at the elevation of 566 m with a downstream slope of 1:0,85 (V:H) and a vertical upstream slope. Considering the normal water level of 585 m, the resulting dam height is 22,8 m.

The main characteristics of the dam are summarized in Table 3.

Table 3 – Main characteristics of the dam body

Type (-)	Concrete/gravity
Crest width (m)	3
Crest length (m)	270
Crest elevation (m)	588,5
Height (m)	22,8

The main characteristics of the reservoir are summarized in Table 4.

Table 4 – Main characteristics of the reservoir

Minimum exploitation level (MEL) (m)	575,5
Normal water level (NWL) (m)	585
Maximum flood level (MFL) (m)	587
Dead storage level (NMorto)	571,3
Normal storage capacity (NSC) (m ³)	775491,4
Minimum storage capacity (MSC) (m ³)	171596,1
Dead storage (VMorto) (m ³)	37500

3.2. Spillway and Bottom Outlet

The spillway is located over the dam body and comprises a WES weir and an energy dissipation structure, known as ski-jump designed according to VICHER & HAGER (1998). The main characteristics are shown in Table 5.

Table 5 – Characteristics of the spillway

Peak flow discharge (m ³ /s)	65,00
Design head (m)	2,00
Width (m)	10,00
Discharge coefficient (m)	0,52
Radius bucket (m)	2,76
Angle bucket (°)	95,7
Take off angle jet (°)	30
Width ski jump (m)	5

The bottom outlet encompasses an upstream trashrack, an upstream plan gate, a transition, a steel pipe, a reduction cone and a Howell Bunger valve.

The bottom outlet entrance was established at the elevation of 568,5 m, 2 m above the NMorto (Table 4) and it is connected to a steel pipe with a diameter of 0,8 m. In the end of the pipe there is Howell-Bunger valve with a diameter of 0,4 m.

In the preliminary design of the bottom outlet, it was considered that, in order to completely empty the reservoir seven days would be required with a discharging rate of 1,38 m³/s.

The trashrack and the plan gate areas were designed according to the maximum cross-sectional flow velocities. The main characteristics of the bottom outlet can be seen in the Table 6.

Table 6 - Main characteristics of the bottom outlet

Bottom outlet entrance (m)	568,5
Discharge (m ³ /s)	1,28
Steel pipe diameter (m)	0,8
Steel pipe length (m)	18,14
Trashrack area (m ²)	1,5 x 1,5
Plan gate area (m ²)	1x1
Valve diameter (m)	0,4

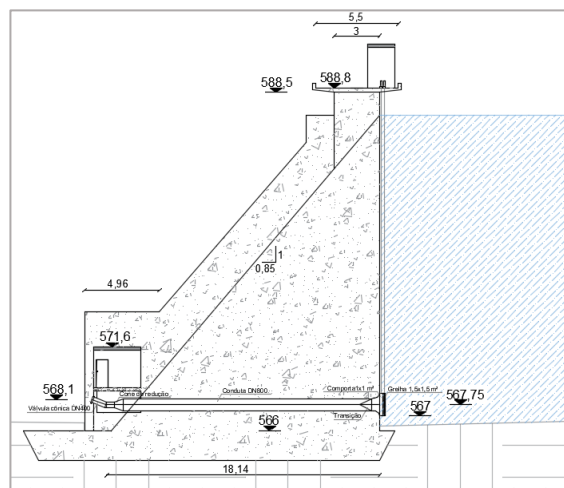


Figure 1 – Bottom outlet. Longitudinal section

3.3. Water intake and Hydraulic circuit

The water intake comprises several elements such as the upstream trashrack, the upstream gate, the air conduit, the second gate, the steel

pipe, the transition section from rectangular to circular.

Due to the minimum submersion (2,3 m) concerning the MEL, the intake entrance is positioned at the elevation of 571, 8 m. The water intake was specifically designed for 3 m³/s (Table 7).

Table 7 – Main characteristics of the water intake

Intake entrance (m)	571,8
Discharge (m ³ /s)	3
Steel pipe diameter (m)	1,4
Trashrack area (m ²)	1,8x1,8
Trashrack thickness (m)	0,3
Plan gate area (m ²) (x2)	1,4x1,4
1 st Plan gate thickness (m)	0,3
2 nd Plan gate thickness (m)	0,2
Air conduit (m)	0,2

In general, the turbine/pump operation mainly share the same pipeline, a penstock with 1,4 m of diameter which connects the dam intake and the powerhouse. The first branch of the pipeline crosses a 1,7 km concrete tunnel with 1% slope until it reaches the surface at the elevation of 555,47 m. Then, the penstock continues at surface until it reaches a bifurcation that separates the pump circuit from the turbine circuit. The penstock characteristics are detailed in Table 8.

Table 8 – Preliminary design of the penstock

Flow (m ³ /s)	3
Diameter (m)	1,4
Section velocity (m/s)	2
Thickness (mm)	12

The turbine circuit encompasses a reduction cone, a DN800 penstock with 10,86 m and a sphere valve, whereas the pump circuit comprises: a DN1400 penstock with 21,79 m

which bifurcate due to the two installed pumps; two DN1000 penstock with 27,16 m; two reduction cones; two DN600 penstock with 2,3 m and downstream of the pumps, a sphere valve and a non-return valve.

The river water captation is made through four water intakes, each of which comprises a trashrack (1x1 m²), a plan gate (1x1m²), a section transition, a concrete conduit and a steel pipe connected to the pump, both with a diameter of 0,6 m.

The intake entrance collected the river water at a rate of 0,75 m³/s and it was set at the elevation of 117,19 m. The facilities' layout can be seen in Figure 2 and Figure 3.

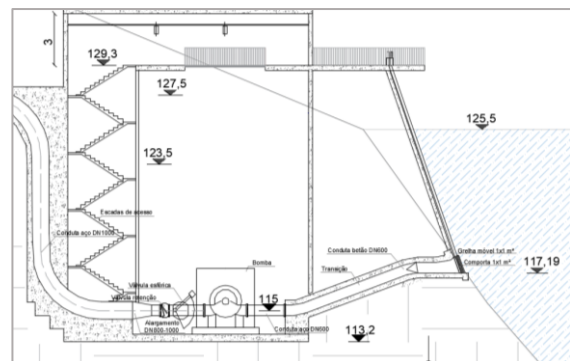


Figure 2 - Water intake of the powerhouse (Longitudinal section)

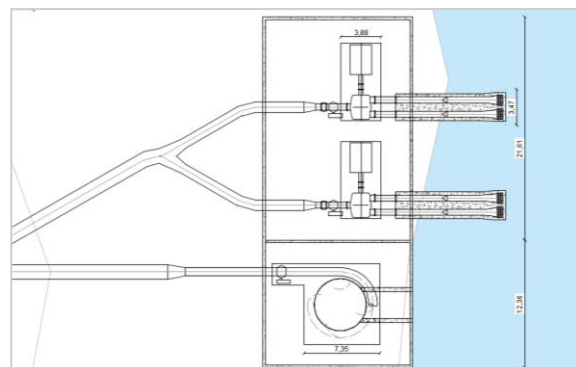


Figure 3 – Powerhouse with a Pelton turbine and the two pumps installed (Plant).

4. Generation System

The generation system consists of a hydropower plant, wind farm and a conventional power station (CPS). The hydropower plant includes a 11,37 MW Pelton turbine that operates under a net head of 455,05 m at a flow rate of 3 m³/s and two 7,93 MW centrifugal pumps with both operating under a manometric head of 464,95 m at a flow rate of 1,5 m³/s.

The conventional power station comprises a diesel engine, with a total installed capacity of 9,5 MW for the purpose of assisting the hydro-wind system in case of the wind and hydroelectric power generation fails to attend the demand. The wind farm includes several wind turbines, each of which with an installed capacity of 2,05 MW. The series of wind power production was provided by Laboratório de Energia e Geologia (LNEG).

The demand series, also provided by LNEG, has the peak demand of 9,5 MW.

Table 9 summarizes the main characteristics of the turbine and the pumps.

Table 9 – Characteristic of the Pelton Turbine and the Centrifugal Pump

Pelton Turbine	Net Head (m)	455,05
	Efficiency (%)	85
	Flow (m ³ /s)	3
	Rotation speed (rpm)	7500
	Power (MW)	11,27
	Elevation axis (m)	127,5
	nozzle diameter (m)	0,8
	shaft	vertical
Centrifugal Pump	Net Head (m)	464,95
	Efficiency (%)	86,2
	Flow (m ³ /s)	1,5
	Rotation speed (rpm)	1500
	Discharge diameter (m)	0,6
	Suction diameter (m)	0,6
	Stages	2

Power (MW)	7,93
NPSH (m)	20
Elevation axis (m)	115
Suction nozzles	2
shaft	horizontal

5. Model and Simulation

The model essentially receives as inputs the electrical demand and the wind energy production generating an order to produce addition energy (hydro energy or/and diesel energy) or to store the excess of the wind energy by pumping. The produced or stored energy generates a flow response (turbined flow or pumped flow) according with the equation (1) and (2), respectively.

$$P_T = \eta_T \gamma Q H_T \quad (1)$$

$$P_P = \gamma Q H_P / \eta_P \quad (2)$$

where:

- P_T, P_P Electrical powers of hydro turbine and pumps;
- Q_T, Q_P Discharge rates of hydro turbine and pumps;
- H_T, H_P Hydraulic heads of hydro turbine and pumps;
- η_T, η_P Turbine and pump efficiencies;
- γ Specific weight.

Therefore, the stored volume in the reservoir at the end of each time step t+1 relates with the volume at the beginning of the time step t and with the inflows and outflows volumes between t and t + 1 according the mass balance equation (3).

$$\frac{dV}{dt} = Q_a + Q_e \quad (3)$$

$$V_{t+1} = V_t + \left(\frac{Q_a_t + Q_a_{t+1}}{2} - \frac{Q_e_t + Q_e_{t+1}}{2} \right) \Delta t$$

The Q_a embodies the inflows, such as the natural daily inflows and the pumped flow, whereas the

Q_e represents the outflows, namely, the ecological discharge, the flood discharge, the evaporation flow and the turbinated flow.

Apart from the flood discharge, the turbinated flow and the pumped flow, the remained series were defined by the hydrological study.

Additionally, the model runs two subroutines:

- I. Subroutine for the estimation of the volume and water level according to the storage capacity curve;
- II. Subroutine for the estimation of flood discharge according with the flow curve of the spillway,

If the difference between the wind-generated electrical power and the hourly electricity demand are negative, the energy deficit will be covered by hydropower generation, which generates turbinated flow.

In the event of the power generated by the wind farm overcomes the energy demand, the pumps start operating by raising the water from the river to the upper reservoir, in which case the hydropower plant generates a pumped flow.

However, there are technical restrictions such as the maximum and minimum water discharge rate both turbine and pump, the storage capacity (MFL) and the minimum level of exploitation (MEL) of the reservoir. Regarding pumps operation the minimum discharge rate is 15% of the project discharge, whereas in the turbine operation this is 20%. The CPS starts to generate in case of the water level in the reservoir reaches the MEL or to provide an amount of energy that required turbinated flow above the minimum.

In the hourly simulations performed, the reservoirs were assumed to be full at instant 0 and the turbine and pumps efficiencies are

considered constant disregarding the flow or power required.

The programme inputs are:

Q_{nati}	Series of the daily mean discharge (m^3/s);
Q_{eco_i}	Ecological discharge monthly series (m^3/s);
Q_{evap_i}	Evaporation monthly series (m^3/s);
E_{EOL_i}	Annual series of wind energy generation (MW);
D_{EM_i}	Annual series of energy demand (MW);
MFL	Normal water level (m);
NSC	Normal storage capacity (m^3);
SC	Storage capacity curve of the watershed.

Finally, the program outputs are:

Q_{disc_i}	Discharge flood annual series (m^3/s);
Q_{t_i}	Turbinated flow annual series (m^3/s);
Q_{p_i}	Pumped flow annual series (m^3/s);
P_{p_i}	Pumped power annual series (MW);
P_{t_i}	Turbinated power annual series (MW);
V_i	Time series of the water volume variation in the reservoir (m);
N_i	Time series of the water level variation in the reservoir (m);
E_{CPS_i}	Annual series of the conventional power production (MW).

Based on the model developed in this present work, different simulations were performed to select the optimum number of wind turbines and to establish the most convenient dam capacity.

Therefore, three installed capacity (P_{WIND}) of the wind farms were established and simulated giving four different dam capacities, selected according to the storage capacity curve of the watershed (Table 10).

It is well known that giving the Portugal wind condition, the installed capacity of the wind farm must be greater than the hydropower installed capacity and the peak demand.

Table 10 – Cases scenarios

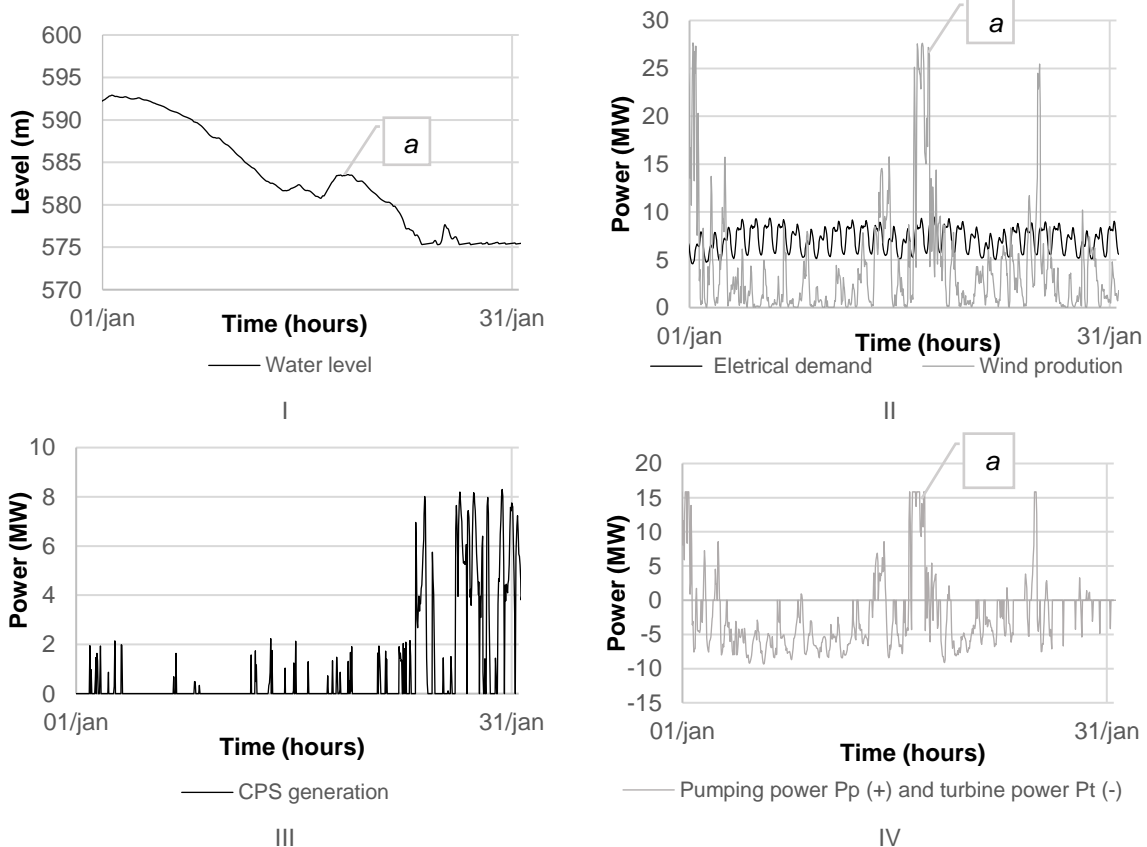
Cases	C1.1	C1.2	C1.3	C1.4	C2.1	C2.2	C3.1	C3.2
P_{WIND} (MW)	20,5	20,5	20,5	20,5	26,65	26,65	30,75	30,75
NSC (m ³)	775491	1249652	2250726	3251800	775491	3251800	775491	3251800
MFL (m)	585	590	595	600	585	600	585	600

For instance, Graphics 3 (I) shows January simulation results of the water accumulation in the reservoir, according to the wind power generation and the demand (II), the pumping and turbine power (IV) and the CPS generation (III).

Analyzing (II) demonstrates that the electrical demand remains above of the wind production most of the time (II), requiring the hydro system to operate in pumping mode, causing a modest raise of the water level. At the end of January, the reservoir is empty, reaching the MEL, and the CPS generation must backup the wind production.

During the presented month, the energy demand below the 2,27 MW is secured by the CPS generation, which corresponds to the lower discharge rate that the turbine can operate at.

In the middle of the month, occurs an excess of wind production, marked with an a in Graphics 3, pushing the hydro system to operate in pumping mode, causing a modest raise of the water level. At the end of January, the reservoir is empty, reaching the MEL, and the CPS generation must backup the wind production.



Graphic 3 – I) Water level variation in the reservoir II) Wind production and electrical demand III) CPS generation IV) Pumping and turbine power requirements (Case C3.2)

6. Discussion

Analyzing demand versus the wind production shows that the wind farm is self-sufficient only 1/3 of the year, requiring the rest of the time a second or third energy generator to satisfy the demand. However, in terms of total amount of energy generated, the wind farm does indeed satisfy 50, 55 and 58 % of the annual demand for different scenarios. Table 11 councils the annual energy demand (C_{ONS}^a) and the annual wind production (E_{EOL}^a), for each cases scenario.

Table 11 – Annual energy demand and annual wind production

Scenarios	C_{ONS}^a (GWh)	E_{EOL}^a (GWh)
C1	56,7	43,4
C2	56,7	56,5
C3	56,7	65,2

The parameters in Table 12 are the analysis's results of the different simulated cases:

- i. Contribution of wind generation to the annual demand (Wind %);
- ii. Contribution of wind generation to the annual demand (Hydro %);
- iii. Contribution of wind generation to the annual demand (CPS %);
- iv. Annual excess of wind production non-accumulated (EA_{HID} %);
- v. Annual excess of wind production accumulated (ENA_{HID} %);
 - a. Annual excess of wind production non-accumulated due to storage capacity ($N \geq MFL$).

On the case C1, the annual conventional power production is greater than the annual hydropower production (Table 12), due to the fact that the water level remained most of the year at MEL. Also, due to that, in the course of the year, the dam is always available to accumulate all the excess of energy from the wind farm. The same is true in C2.1, where in the end of the year the dam ends up empty, which is not an acceptable case scenario because it does not guaranty the hydro energy supplies to the next year.

From case C2.2 to C3.2, the CPS contribution begins to be acceptably lower (less than 15%) and the dam is full in the end of the year. In cases C3.1 and C3.2, however, the threshold condition of 85% for the parameter concerning EA_{HID} % is not met, mainly due to the storage capacity limitation, which points towards the fact that the wind farm size may be unsuitable considering the presented dam capacities.

In fact, in terms of hydro generation, C3.2 is not far from the one obtained in C2.2, which indicates that the raise of the wind farm reflects directly on the diminishing of the CPS contribution.

In the limit, considering the purpose was to maximize the hydro-wind system contribution and minimize the CPS contribution, and simply looking at the environmental impact, the C3.3 would be the optimum case scenario. However, C2.2 provides the best compromises between the hydro-wind system contribution and the energy storage percentage

Table 12 – Contribution of the wind farm, Hydropower plant, CPS to the energy demand and excess of wind production

Cases	Generation			EA_{HID} %	ENA_{HID} %	
	Wind %	Hydro %	CPS%	(-)	Total	$N \geq MFL$
C1.1	50%	21%	29%	96%	4%	4%

Cases	Generation			EA _{HID} %	ENA _{HID} %	
	Wind %	Hydro %	CPS%	(-)	Total	N≥MFL
C1.2	50%	23%	27%	99%	1%	0%
C1.3	50%	25%	26%	99%	1%	0%
C1.4	50%	27%	24%	99%	1%	0%
C2.1	55%	28%	17%	79%	21%	19%
C2.2	55%	33%	12%	94%	6%	3%
C3.1	58%	29%	13%	65%	35%	29%
C3.2	58%	34%	8%	77%	23%	16%

7. Conclusion

In this paper, it was considered a wind-hydro-pumped storage system backed up by a CPS, operating in an isolated grid. The present work aimed, not to design the wind farm, but to design the hydropower enterprises. The main conclusion achieved are the following:

- The natural inflow is not sufficient to ensure the water level, so this must be equalized by the inflow and outflow, by influencing the wind farm and the demand;
- The wind farm installed capacity must be much higher than the hydro installed capacity and the peak demand. Better results in terms of hydro generation were revealed on wind farms with 2,8-3,2 times more than the peak demand;
- Successively raising the installed capacity of the wind farm was enough to annulate or diminish conveniently the CPS contribution, giving that there is a time frame that the wind electrical generation is continuously low according with the wind production data, pushing the water level in reservoir to the MEL;
- C2.2 is the optimum scenario which comprises a 26,65 MW wind farm, a

11,37 MW turbine, a pumped system with an installed capacity of 15,86 MW, and a reservoir with a storage capacity of 3251 800 m³.

In general, given the previous results, the best way to integrate hydro power generation and wind power generation would be to enlarge the store capacity of the dam, considering that a big part of the non-accumulated energy came from the N≥MFL condition (Table 12). That will allow to storage more water to further turbine and confine the CPS contribution to cover the technical limitation of the turbine.

Considering the results, the hydro power plant should be more flexible to higher ranges of turbine discharge flows and have higher number of turbines with less installed capacity, to lower the bottom value of the turbine technical restriction. Also, the installed capacity of the generation system should be close to the pumped system, to minimize the energy loss in the pumped-turbined cycle.

Finally, to further developments, economic and environmental assessments must be conducted to evaluate the benefits of the presented cases scenarios, namely in terms of CO₂ emissions avoided.

References

BRANDÃO, C., RODRIGUES, R. & COSTA, J. P., Análise de fenómenos extremos. Precipitações intensas em Portugal Continental. Direcção dos Serviços de Recursos Hídricos, DSRH- INAG, Lisboa, 2010.

MARTINS, A., Quantificação do efeito da evaporação no dimensionamento da capacidade útil de albufeiras, Dissertação para obtenção de grau de Mestre em Engenharia Civil, Instituto Superior Técnico, 2016.

PINHEIRO, A. N., Tomadas de água em albufeiras, Texto de apoio à disciplina de Estruturas Hidráulicas, Departamento de Engenharia Civil, Instituto Superior Técnico, Lisboa, 2006a.

PINHEIRO, A. N., Descarregador de cheias em canal de encosta, Texto de apoio à disciplina de Estruturas Hidráulicas, Departamento de Engenharia Civil, Instituto Superior Técnico, Lisboa, 2006b.

PORTELA M.M., Folhas de apoio à disciplina de Modelação e Planeamento e Recursos Hídricos, 4º ano semestre 2007/2008, Departamento de Engenharia Civil, Instituto Superior Técnico, 2007.

PORTELA M.M., Slides de apoio à disciplina de Hidrologia e Recursos Hídricos, p. 213 a 293, Departamento de Engenharia Civil, Instituto Superior Técnico, 2013.

PORTELA, M. M. & HORA, G., Aplicação da fórmula racional à análise de cheias em Portugal Continental: valores do coeficiente C, In "Congresso da Água", Porto, 2002.

ROCHA, J. S., Assoreamento das Albufeiras e o Ambiente, LNEC, Seminário Barragens e Ambiente, Porto, 1998.

BUREAU OF RECLAMATION (BUREC), Design of small dams, 3ª edition, Water Resources Technical Publication, Washington, 1987.

HIPÓLITO, J. R., & VAZ, A. C., Hidrologia e Recursos Hídricos, 1ª Edição, IST Press, Lisboa, 2011

LENCASTRE, A., Hidráulica geral, 1983.

QUINTELA, A. C., Hidráulica, 9ª Edição, Fundação Calouste Gulbenkian, 1996.

RAMOS, H., ALMEIDA, A. B., PORTELA, M., & ALMEIDA, H. P., Guidelines for design of small hydropower plants, WREAN and DED, Belfast, North Ireland, 2000.

VISCHER, D. L. & HAGER, W. H., Dam Hydraulics, 1ª Edição, WILEY, Zurich, Switzerland, 1998.